NJC

PAPER

View Article Online
View Journal | View Issue

Cite this: *New J. Chem.*, 2018, **42**, 214

The effect of alkyl chain tethers on the kinetics and mechanistic behaviour of bifunctional dinuclear platinum(II) complexes bearing *N,N′*-dipyridylamine ligands†

Panyako Asman Wangoli *[a] and Grace Kinunda[b]

In the current paper, we report the kinetics of bifunctional dinuclear platinum(II) complexes *viz.*, 1,2-*N,N′*-di-(2,2-dipyridylamine)ethanetetraaquaplatinum(II), **PtL2**, 1,3-*N,N′*-di-(2,2-dipyridylamine)propanetetraaquaplatinum(II), **PtL3**, 1,4-*N,N′*-di-(2,2-dipyridylamine)butanetetraaquaplatinum(II), **PtL4**, 1,5-*N,N′*-di-(2,2-dipyridylamine)pentanetetraaquaplatinum(II), **PtL5** and 1,6-*N,N′*-di-(2,2-dipyridylamine)hexanetetraaquaplatinum(II), **PtL6**. The substitution reactions were carried out on tetraaqua complexes with thiourea nucleophiles under pseudo-first-order conditions as a function of nucleophile concentration and temperature by stopped-flow and UV-vis spectrophotometric techniques. An experimental study was conducted with the aim of determining the influence of alkyl chains on the steric and electronic structure of dinuclear platinum(II) complexes. The reactivity of these complexes was dependent on the length of the alkyl spacer. The results obtained herein demonstrate the intriguing odd–even effects induced by the alkyl chain on the complexes. Artificial constraints imposed by the alkyl chain significantly affect their conformational structure to be either synperiplanar (*syn*-) or antiperiplanar (*anti*-) characterized by the odd and even effect. The kinetic, mechanistic and conformational behaviour was influenced by the size of the alkyl chain in accordance with odd–even alterations of the spacer. Computational modeling using density functional theory (DFT) calculations supplemented experimental findings that structural features and the reactivity pattern of these organometallic complexes are governed by both steric and electronic effects arising from the flexibility and inductive nature of the alkyl spacer. The strong σ-donicity of longer alkyl chains favours sufficient accumulation of electron density at the metal centre and stabilizes a 14-electron intermediate. The study shows the HOMO–LUMO energy (ΔE) is affected by the length of the spacer. Kinetic and DFT data indicate electron donation by the alkyl spacer. The low positive values of enthalpy of activation and significantly large negative values of entropy of activation indicate an associative mechanism of substitution.

Received 14th August 2017,
Accepted 10th November 2017

DOI: 10.1039/c7nj03021e

rsc.li/njc

Introduction

Although platinum based-drugs, such as cisplatin, oxaliplatin and carboplatin have become the mainstays of cancer chemotherapy, problems of resistance and side effects that include severe ototoxicity, neurotoxicity,[1–5] nausea, vomiting and nephrotoxicity[6,7] have limited their clinical use. This has motivated the development of other platinum anticancer drugs that are less toxic, with less cross resistance and with a broader spectrum of activity.[8–10] Novel platinum(II) drugs, distinctive from cisplatin and its analogues in terms of the structure and nature of Pt–DNA adducts, are viewed to improve the biological profile of platinum anticancer agents by circumventing or complementing cisplatin specific biological processes in DNA repair. This study is in search for new multinuclear platinum(II) complexes which represent a completely new paradigm shift in the development of novel anticancer agents.[11–13]

Multinuclear complexes contain two or more platinum centres that can bind to DNA forming long range flexible and non-directional DNA adducts that induce DNA conformational changes.[14–17] This has been shown by complexes bridged by aliphatic diamines showing higher cytotoxic activity in cisplatin-resistant

[a] *School of Chemistry and Physics, University of KwaZulu-Natal, 3209, Scottsville, Pietermaritzburg, South Africa. E-mail: pwangoli@yahoo.com*
[b] *Department of Chemistry, University of Dar es Salaam, P.O. Box 35061, Dar es Salaam, Tanzania*

† Electronic supplementary information (ESI) available: Selected wavelengths used for kinetic measurements, tables of observed pseudo-first-order rate constants, Eyring plots, mass spectrometry: mass spectral data showing respective molecular ions and their fragmentation patterns, NMR data for ^{1}H NMR, ^{13}C NMR and ^{195}Pt NMR, pK_a titration spectra of the complexes. See DOI: 10.1039/c7nj03021e

cell-lines.[10,12,14,18–20] Complexes of this class have overcome both acquired and intrinsic resistance due to their ability to form long range DNA adducts.[9–12] The amphiphilic nature of the amine linkers, coupled with charge dispersion along their carbon backbone, results in an enhanced cellular uptake of the anticancer drug. This cytotoxic potency of these anticancer agents is strictly regulated by their electronic and structural conformations.[21,22] These characteristic variations are attributed to the coordinating ligands that connect platinum nuclei.[23–27] The best activity for such a class of complexes has been reported for BBR3464, $[\{trans\text{-}PtCl(NH_3)_2\}_2\{\mu\text{-}trans\text{-}Pt(NH_3)_2(H_2N(CH_2)_6NH_2)_2\}]^{4+}$, (1,0,1/t,t,t), the first trinuclear bifunctional DNA binding agent to undergo phase II clinical trials. Furthermore, it is also the first and only non-cisplatin analogue introduced into the human body.[28–32] Although multinuclear complexes have been reported to prevent tumour growth, their exact underlying molecular and kinetic mechanisms remain unexplored.

To provide information on the substitution mechanisms of dinuclear Pt(II) complexes and to estimate their reactivity inside the cell, determination of substitution kinetics remains vital. Furthermore, kinetic studies are of interest to shed light on the complex metabolism and predict treatment response in cancer patients.[33] For the first time, the current study investigates the substitution reactions of tetraaqua dinuclear Pt(II) complexes having a $[cis\text{-}Pt(N,N')(H_2O)_2]$ molecular structure with an alkyl backbone that mimic cisplatin. This is with the view that Pt(II) complexes with *cis* geometry have a higher efficacy in antitumour cell lines than those with *trans*-geometry. To obtain these complexes, a series of 2,2′-dipyridylamine chelates appended to alkyl chain tethers of variable lengths (n = 2–6) were used. The only variable was the $-(CH_2)_n-$ moiety in the spacer which allowed the effect of the alkyl chain on the behaviour of the complexes with *cis*-geometry to be probed.

These compounds may be useful to gain more insights into how these Pt(II) complexes interact with bio-relevant molecules and enable them to be applied as antitumour agents. Their substitution reaction with thiourea nucleophiles was investigated. This class of nucleophiles was of interest due to their role as chemoprotective agents.[34–37] The nucleophiles *viz.* thiourea (TU), *N*,*N*′-dimethylthiourea (DMTU) and *N*,*N*,*N*′*N*′-tetramethylthiourea (TMTU) were chosen as representatives of the targets and competitors[38] of platinum drugs in the cellular environment. They have strong affinity towards the platinum centre and good solubility. Also their relatively fast reactivity with Pt(II) complexes makes this set of nucleophiles convenient for preliminary experiments.[39–41a] Scheme 1 shows the complexes investigated while a mononuclear dipyridylamine complex **PtL1***, from the literature,[41b] was included for comparison purposes.

Experimental section

Materials and methods

All starting materials were of analytical grade and were obtained from commercial sources and used without further purification. The nucleophiles thiourea (TU, 99%), *N*,*N*′-dimethylthiourea (DMTU, 99%) and *N*,*N*,*N*′*N*′-tetramethylthiourea (TMTU, 98%) and the starting materials 1,2-diiodoethane, 99%, 1,3-diiodopropane, 99%, 1,4-diiodobutane, 99%, 1,5-diiodopentane, 97%, 1,6-diiodohexane, 97%, and $AgClO_4$ 99.99% were obtained from Sigma Aldrich. K_2PtCl_4 and 2,2′-dipyridylamine (dpa) were obtained from Strem Chemicals. De-ionized water was used in all experiments.

Synthesis of the ligands

1,2-*N*,*N*′-Di-(2,2′-dipyridylamine)ethane (**L2**), 1,3-*N*,*N*′-di-(2,2′-dipyridylamine)propane (**L3**), 1,4-*N*,*N*′-di-(2,2′-dipyridylamine)-butane (**L4**), 1,5-*N*,*N*′-di-(2,2′-dipyridylamine)pentane (**L5**) and 1,6-*N*,*N*′-di-(2,2′-dipyridylamine)hexane (**L6**) were synthesized

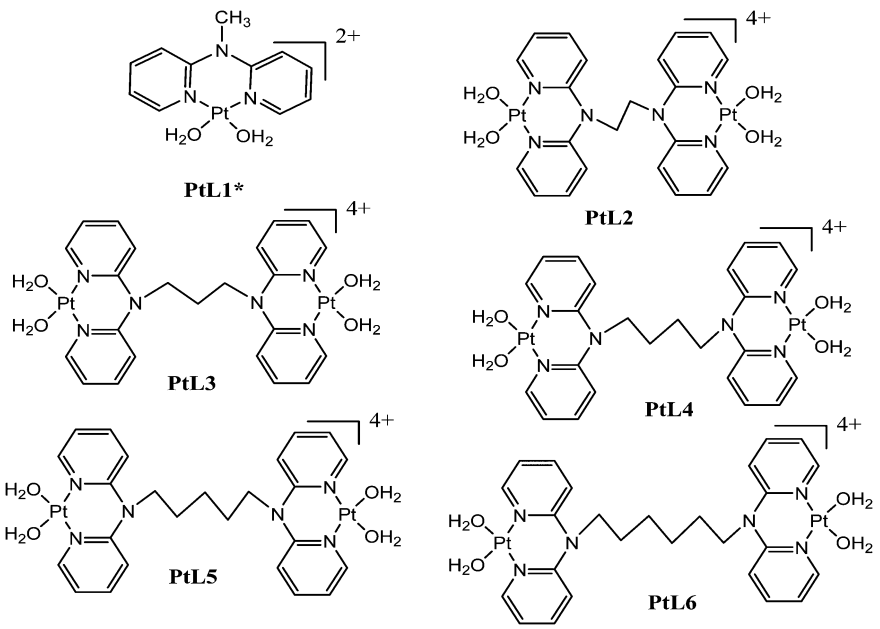

Scheme 1 Chemical structures of the investigated Pt(II) complexes.

following a reported procedure by Krebs *et al.*[42] To a suspension of KOH (0.023 mol, 1.30 g) in 30 mL of DMSO, 2,2′-dipyridylamine (dpa) (5.00 mmol, 0.856 g) was added. The suspension was stirred at room temperature for 24 h and the respective linker, α,ω-iodoalkane (2.5 mmol), was added drop-wise. The mixture was stirred for another 5 hours and quenched with 50 mL of water thereafter. The desired products were extracted with chloroform (4 × 30 mL) and the organic layer was dried over anhydrous magnesium sulphate. The solvent was removed under reduced pressure and the product was recrystallized from a dichloromethane/hexane mixture to obtain pure solids or oil. These ligands were characterized using ^{1}H, ^{13}C, NMR, mass spectroscopy and elemental analysis.

L2, yield: 548.3 mg, 60% (white needle crystalline powder). ^{1}H NMR (400 MHz, $CDCl_3$): δ 8.26 (dd, 4H), 7.60 (dd, 4H), 7.55 (td, 4H), 6.85 (dd, 4H), 1.78 (brs, 4H). ^{13}C NMR (400 MHz, $CDCl_3$): 154.0, 147.8, 137.8, 116.4, 111.7 and 41.0. Anal. calcd for $C_{22}H_{20}N_6$: C 71.74, H 5.43, N 22.83; found: C 72.12, H 5.28, N 23.18, TOF MS ES$^+$: m/z = $[M + H]^+$ = 369.452.

L3, yield: 577.8 mg, 60% (yellow needle crystalline powder). ^{1}H NMR (400 MHz, $CDCl_3$): δ 8.24 (dd, 4H), 7.58 (dd, 4H), 7.54 (t, 4H), 6.83 (dd, 4H), 4.19 (brs, 2H), 2.04 (brs, 4H). ^{13}C NMR (400 MHz, $CDCl_3$): 154.4, 148.3, 138.3, 116.9, 112.2, 41.5 and 25.8. Anal. calcd for $C_{23}H_{22}N_6$: C 72.25, H 5.76, N 21.99; found: C 72.52, H 5.56, N 21.72, TOF MS ES$^+$: m/z = 383.1987 $[M + H]^+$.

L4, yield: 601.9 mg, 61% (yellow cubic like crystals). ^{1}H NMR (400 MHz, $CDCl_3$): δ 8.30 (dd, 4H), 7.48 (dd, 4H), 7.03 (t, 4H), 6.82 (dd, 4H), 4.19 (m, 4H), 1.76 (brs, 4H). ^{13}C NMR (400 MHz, $CDCl_3$): 157.5, 148.4, 137.1, 116.9, 114.9, 48.1 and 25.8. Anal. calcd for $C_{24}H_{24}N_6$: C 72.73, H 6.06, N 21.21; found: C 73.11, H 6.40, N 21.17, TOF MS ES$^+$: m/z = 419.1791 $[M + Na]^+$.

L5, yield: 628.3 mg, 61% (yellow oil). ^{1}H NMR (400 MHz, $CDCl_3$): δ 8.18 (dd, 4H), 7.37 (dd, 4H), 6.94 (d, 4H), 6.70 (dd, 4H), 4.03 (m, 4H), 1.62 (m, 2H), 1.27 (m, 4H). ^{13}C NMR (400 MHz, $CDCl_3$): 157.4, 148.3, 137.1, 116.8, 114.6, 48.4, 28.1 and 24.6. Anal. calcd for $C_{25}H_{26}N_6$: C 73.17, H 6.34, N 20.49; found: C 73.13, H 5.93, N 20.87, TOF MS ES$^+$: m/z = 411.2292 $[M + H]^+$.

L6, yield: 653.0 mg, 63% (yellow oil). ^{1}H NMR (400 MHz, $CDCl_3$): δ 8.13 (dd, 4H), 7.33 (dd, 4H), 6.88 (d, 4H), 6.66 (dd, 4H), 4.25 (m, 4H), 1.49 (m, 4H), 1.40 (m, 4H). ^{13}C NMR (400 MHz, $CDCl_3$): 157.4, 148.2, 137.0, 116.8, 114.6, 48.2, 28.1 and 26.8. Anal. calcd for $C_{26}H_{28}N_6$: C 73.58, H 6.60, N 19.81; found: C 73.24, H 6.34, N 20.44, TOF MS ES$^+$: m/z = 425.2441 $[M + H]^+$.

Preparation of the platinum(II) complexes

The chloro forms of the Pt(II) complexes were synthesized using a general procedure reported by Krebs *et al.*[42] To a stirred solution of K_2PtCl_4 (0.5 mmol, 0.2075 g) in 50 mL of water, a solution of alkyl diamine (0.25 mmol) of the bridging spacer dissolved in 10 mL of ethanol was added dropwise. The reaction mixture was then refluxed at 50 °C for 24 h. The resulting yellow precipitates were filtered off, washed with ultrapure water, ethanol and diethyl ether and dried in a vacuum.

PtL2, yield: 165.5 mg, 74%. ^{1}H NMR (400 MHz, DMSO-d_6): δ 8.77 (dd, 4H), 7.97(dd, 4H), 7.29 (dd, 4H), 7.11 (ddd, 4H), 2.53 (brs, 4H). ^{13}C NMR (400 MHz, DMSO-d_6): 151.6, 151.0, 141.9, 119.6, 120.4 and 19.7. Anal. calcd for $C_{22}H_{20}Cl_4N_6Pt_2$: C 29.33, H 2.22, N 9.33; found: C 29.64, H 2.81, N 9.15.

PtL3, yield: 159.2 mg, 70%. ^{1}H NMR (400 MHz, DMSO-d_6): δ 8.24 (dd, 4H), 7.58 (dd, 4H), 7.54 (t, 4H), 6.83 (dd, 4H), 4.19 (brs, 2H), 2.04 (brs, 4H). ^{13}C NMR (400 MHz, DMSO-d_6): 154.4, 148.3, 138.3, 116.9, 112.2, 41.5 and 25.8. Anal. calcd for $C_{23}H_{22}Cl_4N_6Pt_2$: C 30.20, H 2.41, N 9.19; found: C 29.94, H 2.25, N 8.99.

PtL4, yield: 152 mg, 66%. ^{1}H NMR (400 MHz, DMSO-d_6): δ 8.78 (dd, 4H), 8.05 (dd, 4H), 7.51 (d, 4H), 7.24 (dd, 4H), 4.23 (brs, 4H), 1.96 (brs, 4H). ^{13}C NMR (400 MHz, DMSO-d_6): 153.9, 152.6, 142.4, 122.7, 117.9, 50.5 and 25.1. Anal. calcd for $C_{24}H_{24}Cl_4N_6Pt_2$: C 31.03, H 2.59, N 9.05; found: C 30.90, H 2.76, N 8.18.

PtL5, yield: 156.5 mg, 66%. ^{1}H NMR (400 MHz, DMSO-d_6): δ 8.81 (dd, 4H), 8.03 (dd, 4H), 7.49 (d, 4H), 7.27 (dd, 4H), 4.16 (t, 4H), 1.91 (m, 2H), 1.72 (m, 4H). ^{13}C NMR (400 MHz, DMSO-d_6): 153.4, 151.8, 141.6, 121.9, 117.1, 50.2, 31.3 and 26.5. Anal. calcd for $C_{25}H_{26}Cl_4N_6Pt_2$: C 31.85, H 2.76, N 8.92; found: C 32.27, H 2.80, N 8.17.

PtL6, yield: 145.7 mg, 61%. ^{1}H NMR (400 MHz, DMSO-d_6): δ 8.79 (dd, 4H), 8.06 (dd, 4H), 7.54 (d, 4H), 7.26 (dd, 4H), 4.15 (br, 4H), 1.65 (m, 8H). ^{13}C NMR (400 MHz, DMSO-d_6): 154.2, 152.6, 142.4, 122.4, 118.1, 50.8, 32.1 and 28.3. Anal. calcd for $C_{26}H_{28}Cl_4N_6Pt_2$: C 32.63, H 2.93, N 8.79; found: C 32.95, H 2.89, N 8.34.

Instrumentation and physical measurements

NMR characterization of the ligands and complexes was performed on a Bruker Avance III 500 or a Bruker Avance 400 spectrometer at frequencies of 400 MHz and 125 MHz/100 MHz using either a 5 mm BBOZ probe or a 5 mm TBIZ probe at 30 °C with chemical shifts referenced to the relevant solvent signal. Mass analysis was done on a Waters Micro-mass LCT Premier Spectrometer and elemental analysis on a Thermo Scientific Flash 2000. Kinetic studies for fast reactions were monitored using an Applied Photophysics SX20 Stopped-Flow spectrophotometer coupled to an online data acquisition system, and a Varian Cary 100 Bio UV-visible spectrophotometer thermostated using a Varian Peltier temperature controller to within ±0.05 °C was used for the slow kinetic measurements. The kinetic traces were analyzed using the Origin 7.5® software package.[43] The pH of the solutions was recorded on a Jenway 4330 conductivity/pH meter. The pH meter was calibrated using standard buffer solutions at pH values of 4.0, 7.0 and 10.0.

Preparation of solutions for kinetic analysis

Due to the low solubility of the chloro complexes in kinetic solutions, they were converted to their aqua analogues according to a literature procedure.[44–47] The solutions of the aqua complexes were prepared by the reaction of a known amount of the chloro Pt(II) complex with $AgClO_4$ in a molar ratio of 1 : 3.98 in 0.1 M $HClO_4$. The mixture was stirred at 40–50 °C for 48 h in the dark to protect it from light. After cooling the AgCl precipitate was removed by filtration through a 0.45 μm pore

membrane filter. The filtrate was diluted with 0.1 M $HClO_4$ solution to final concentrations of the respective complex solutions.

pK_a determination of the aqua complexes

The acidity of the aqua ligands coordinated to the metal centre was determined by spectrophotometric titration to obtain pK_a values. This method was preferred due to its ability to give a titration curve that enables the estimation of the pK_a values. Spectrophotometric measurements were performed on a Varian Cary 100 Bio UV-visible spectrophotometer thermostated using a Varian Peltier temperature controller to within ±0.05 °C in the wavelength range 200–800 nm (visible spectrum). The pH measurements were recorded on a Jenway 4330 conductivity/pH meter. Large volumes of the platinum aqua complex (300 mL) were used during titration to avoid absorbance corrections due to dilution. NaOH was used as the base for spectrophotometric titration in the pH range of 1–10 at 25 °C. Crushed NaOH pellets were used in the pH range of 1–3 after which Pasteur pipettes were used for dropwise addition of 0.5 M, 0.1 M, 0.05 M and 0.001 M of NaOH solution. After addition of the base, samples of about 500 μL were taken in ampoules and their pH was recorded. After determining the pH the samples in the ampoules were discarded to avoid possible chloride ion contamination from the pH electrode. 2.0 mL solution of the platinum aqua complex was placed in a cuvette for UV/vis spectrophotometric pH titration with NaOH as a base. The plots of absorbance *versus* pH at a specific wavelength were used to determine the pK_a values of the coordinated aqua ligands. The data obtained were fitted to separate single sigmoidal functions by the Boltzmann equation using the Origin 7.5® software. A classic example of a sigmoid curve plotted as absorbance *versus* pH to determine the pK_a values is illustrated in Fig. S41 in the ESI.† Fig. S39 and S40 (ESI†) shows typical sigmoid curves obtained from the complexes. The inflection point corresponds to the pK_a value reported in the study. The titration data for the complexes were fitted to the sigmoid curve using the Boltzmann eqn (2) that showed four stepwise deprotonation values for dinuclear complexes as reported in Table 3.

Kinetic measurements

All kinetic measurements were performed under pseudo-first-order conditions. The nucleophile concentration was at least a 40-fold excess compared to that of the Pt(II) complexes in all reactions. This ensured at least 10-fold of nucleophile concentration at each platinum centre and hence forced the reaction to completion. Spectral changes resulting from mixing the dinuclear Pt(II) complex and nucleophile solutions were recorded over the wavelength range 200 to 800 nm to establish a suitable wavelength at which kinetic measurements could be performed. A summary of the wavelengths used for each nucleophile is presented in Table S1 in the ESI.† The temperature was controlled throughout all kinetic experiments within an accuracy of ±0.05 °C. For the determination of the activation parameters (enthalpies and entropies) the rate of the reaction was measured as a function of temperature, over a temperature range of 15 to 40 °C at intervals of 5 °C. The rate constants reported represent an average value of at least six to eight independent kinetic runs for reactions performed on the stopped flow spectrophotometer and of triplicate runs for those followed on the UV-visible spectrophotometer. The k_{obs} values were obtained from nonlinear least-squares by fitting the exponential function in eqn (1) to the time dependent absorbance.[48]

$$A_t = A_\infty + (A_0 - A_\infty)\exp^{(-k_{obs}t)} \quad (1)$$

where A_0, A_t and A_∞ represent the absorbance of the reaction mixture initially, at time t, and at the end of the reaction, respectively. Activation parameters were determined from a linear least-squares analysis of $\ln(k_2/T)$ *versus* $1/T$ using the Eyring plots.

Computational calculations

Computational calculations for parameters such as the chemical potential, chemical hardness and electrophilicity indices, using density functional theory (DFT), were performed with the Gaussian 09 programme suite.[49] Geometrical optimizations were carried at the B3LYP/LanL2DZ level of theory. B3LYP refers to a three parameter functional hybrid exchange of Becke[50] with the functional correlation gradient of Lee, Yang and Parr,[51] whereas LanL2DZ refers to the Los Alamos National Laboratory 2 Double ζ basis set.[52] The singlet states were used due to the low electronic spin of Pt(II) complexes. The aqua complexes were modelled as cations with an overall charge of +4. The optimized structures of frontier molecular orbitals and other key geometrical data are presented in Tables 1 and 2 respectively. The dihedral and basal angles of the complexes were obtained from the optimized structures of the respective complexes as indicated in Fig. 1 and the values are summarized in Table 2.

The two pyridyl rings of each dpa have similar dihedral angles because of similar spatial repulsions. The values of these angles for the complexes are summarized in Table 2. Thus, preorganization is shown by the alkyl chain to impart conformational stability. The preorganization is achieved by the alkyl chain to impose electronic and steric effects that restrict the dihedral angles of dipyridylamines. Although longer alkyl chains are expected to introduce more hindrance to the complexes, similar dihedral and basal angles show that an increase in alkyl chain length provides little steric effect in the immediate vicinity of the platinum atoms. This is in agreement with recent studies on dipyridylamine complexes by Asman and Jaganyi.[53–55] Both current and previous studies give an overview of kinetics and substitution mechanisms of dipyridylamine backbone Pt(II) complexes with sulphur-donor biomolecules to show that they have similar behaviour. The complexes investigated have similarities in structure to cisplatin. Both reviews correlate kinetic, thermodynamic and structural properties of dipyridylamine Pt(II) complexes appended to different chelating ligands. The current and previous studies have contributed to a better understanding of these dipyridylamine Pt(II) complexes with important biomolecules and most likely improve their antitumour activity.

Table 1 DFT optimized geometrical structures of the HOMO and LUMO frontier molecular orbitals of the investigated platinum(II) complexes at the B3LYP/LANL2DZ level of theory (isovalue = 0.02)

Complex	Planarity	HOMO map	LUMO map
PtL2	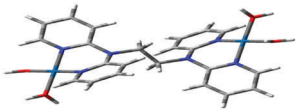	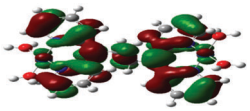	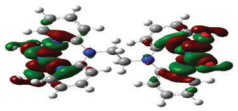
PtL3	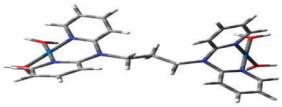	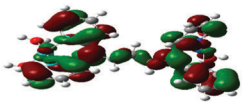	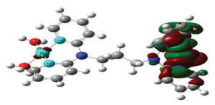
PtL4	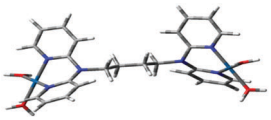	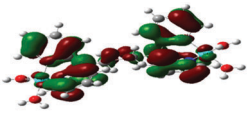	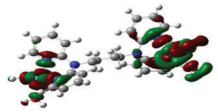
PtL5	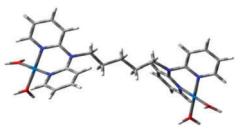	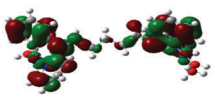	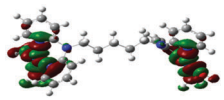
PtL6	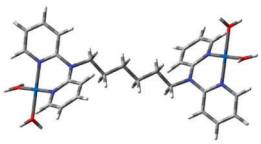	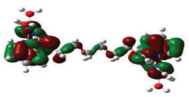	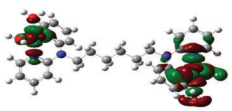

Table 2 Computed bond lengths and angles, natural atomic bond orbital (NBO) charges, and the HOMO–LUMO energy gap for the dinuclear Pt(II) complexes

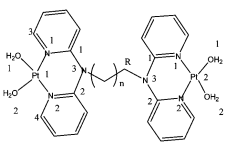

	PtL2	PtL3	PtL4	PtL5	PtL6
HOMO–LUMO energy					
LUMO/eV	−12.33	−11.99	−11.63	−11.37	−11.13
HOMO/eV	−16.66	−16.23	−15.85	−15.52	−15.26
ΔE/eV	4.34	4.24	4.22	4.15	4.13
Electrophilicity index (ω) (eV)	48.44	46.96	44.74	43.49	42.09
NBO charges					
Pt_1	0.776	0.771	0.770	0.767	0.767
Pt_2	0.776	0.771	0.770	0.767	0.767
N_1	−0.517	−0.516	−0.518	−0.518	−0.518
N_2	−0.515	−0.516	−0.517	−0.517	−0.518
N_3	−0.536	−0.513	−0.513	−0.509	−0.509
Dipole moment (Debye)	0.5785	5.5062	3.3977	4.6459	1.3105
Bond length (Å)					
N_3–R	1.4972	1.5004	1.5043	1.5050	1.5067
Pt_1–Pt_2	9.44	9.70	11.58	12.47	14.03
Bond angles (°)					
Dihedral	50.55	50.47	50.28	50.06	50.30
Basal	129.45	129.53	129.72	129.94	129.70

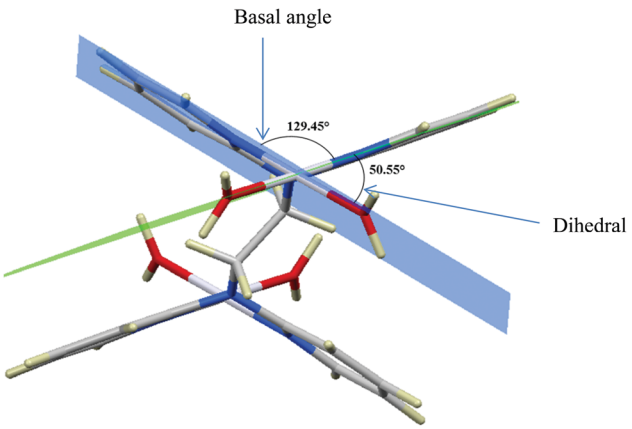

Fig. 1 DFT-optimized structure of **PtL2** showing the dihedral and basal angles between boat conformed pyridyl groups.

Acidity and pK_a titrations of the aqua Pt(II) complexes

The acidity of the complexes in this study is discussed based on the first deprotonation. A typical spectrum obtained during the pH titrations is shown in Fig. 2. From the first deprotonation, the trend for the pK_{a1} values shows that the acidity of the coordinated aqua ligands depends on the length of the alkyl bridge between the metal centres and decreases in acidity as the alkyl chain increases. As was mentioned in the experimental section, the pK_a values were determined from the Boltzmann eqn (2) by fitting a characteristic sigmoid curve and locating the inflection point using the Origin 7.5® software.[43] The pK_a values of the deprotonated complexes are summarized in Table 3 while the proposed deprotonation mechanism is represented in the equilibrium reaction in Scheme 2.

$$y = A_2 + (A_1 - A_2)/(1 + \exp(x - x_0)/\partial x) \quad (2)$$

where A_1 and A_2 are the initial and final y values respectively, x_0 = centre, ∂x = width. The y value at x_0 is half way between the

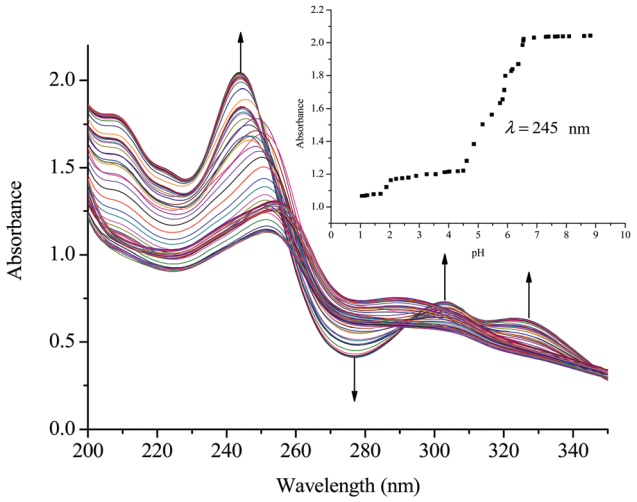

Fig. 2 UV/vis spectral changes for the titration of **PtL2** within the pH range of 1 to 10; the inset shows the titration curve at λ = 245 nm.

two limiting values A_1 and A_2. The y value changes drastically within a range of x variable. The width of this range is approximately ∂x.

The difference in the acidity of dinuclear complexes is attributed to the metal–metal distance through charge addition and also to the inductive effects of the alkyl chain. Complexes with shorter distances between the platinum(II) centres undergo addition of single charges that enhances electrophilicity and acidity due to the close proximity of Pt^{2+} ions.[56] The mutual charge addition of each Pt(II) centre becomes weaker as the distance between the metal centres becomes longer as shown by the current study. This is evident from the pK_{a1} trend in the acidity of the complexes **PtL2** > **PtL3** > **PtL4** > **PtL5** > **PtL6**. The inductive effect of the alkyl group on the pyridine rings is proposed to increase the electron density on the pyridine nitrogen atoms making them stronger donors. The study also suggests that the strength of the inductive effect is dependent on the length of the alkyl chain. The trend shows the longer alkyl chains to stabilize the platinum centres due to their increased inductive effect which is also supported by the slight increase in N_3–R bond lengths across the series as shown in Table 2. As a result, the aqua ligands become more basic and hence have high pK_a values. An increase in electron density around the platinum atom leads to a stronger σ bond and increased intrinsic basicity of the complexes. This increased inductive effect of alkyl moieties enhances the negative charge around platinum centres that results in their stability. This study suggests the inductive effects to be a key factor in the acidity of the complexes. In addition it shows that the dinuclear complexes are more acidic than the mononuclear ones. This difference is attributed to the difference in the overall charge of the complexes which is +2 for the mononuclear and +4 for the dinuclear complexes. Coordination of a second Pt(II) atom results in addition of charges that make the dinuclear platinum complexes more electrophilic that favours aqua deprotonation. Because of the overall charge of +4 on the dinuclear Pt(II) complexes the aqua ligands are more acidic compared to the reference mononuclear complex **PtL1***.

The stability of these complexes is due to each metal centre possessing a delocalized electronic structure with a boat conformation.[42] This makes the Pt centres to be in a conjugated six membered ring that causes the electron density to be delocalized into the ring, hence resulting in the shielding of alkyl protons. The inductive effect of the alkyl group is reported to be transmitted to the Pt(II) centres *via* the lone pair on nitrogen being delocalized over the amide group. The electron lone pair of the nitrogen atom affects cross conjugation of the complexes affecting the stability of Pt(II) centres. As such the NBO charges on the Pt centres do not change significantly since the surrounding environment has identical atomic and conjugative connectivity.[57a] In such complexes, the NBO charge on the metal is not readily quantified due to being in a delocalized system.[57b] Due to the chelating effect the metal ions with a positive charge in the complexes are stabilized through resonance. This behaviour is supported by the raising of frontier orbitals in Table 1. The positively charged Pt^{2+} ion becomes stabilized as the alkyl chain increases indicating increased inductive effect as the alkyl chain length increases.[58,59] This observation is in agreement with the negative charge being stabilized as one moves from $sp^3 \rightarrow sp^2$ closer to the positively charged nucleus. This is also supported by the general decrease in the electrophilicity index across the complexes as the alkyl chain increases. The results also show that the subsequent pK_a values increase with subsequent deprotonation; this observation is attributed to the lowering of the overall charge from +4 to +1. This decrease in the overall charge decreases the electrophilicity and the acidity of the metal centres making it more difficult to deprotonate the consequent coordinated aqua ligand due to the formation of hydroxo species. The pK_a studies show that the complexes undergo four stepwise deprotonation, an observation reported in our previous studies[53–55] and investigations by van Eldik *et al.*[47,60]

Kinetic results

The substitution kinetics of the coordinated aqua ligands in the complexes was followed spectrophotometrically by the change

Table 3 pK_a values for the four stepwise deprotonation equilibria of the tetraaqua Pt(II) complexes

Complex	**PtL1***	**PtL2**	**PtL3**	**PtL4**	**PtL5**	**PtL6**
pK_{a1}	5.24 ± 0.07*	2.11 ± 0.01	2.27 ± 0.01	2.34 ± 0.01	2.47 ± 0.03	2.71 ± 0.06
pK_{a2}	6.19 ± 0.04*	3.74 ± 0.03	3.60 ± 0.01	3.39 ± 0.04	3.44 ± 0.03	3.49 ± 0.01
pK_{a3}	—	4.89 ± 0.04	4.58 ± 0.02	4.88 ± 0.01	4.68 ± 0.05	4.74 ± 0.04
pK_{a4}	—	6.45 ± 0.01	6.38 ± 0.01	6.53 ± 0.02	6.33 ± 0.06	7.04 ± 0.06

pK_a values for **PtL1*** were obtained from ref. 41*b*.

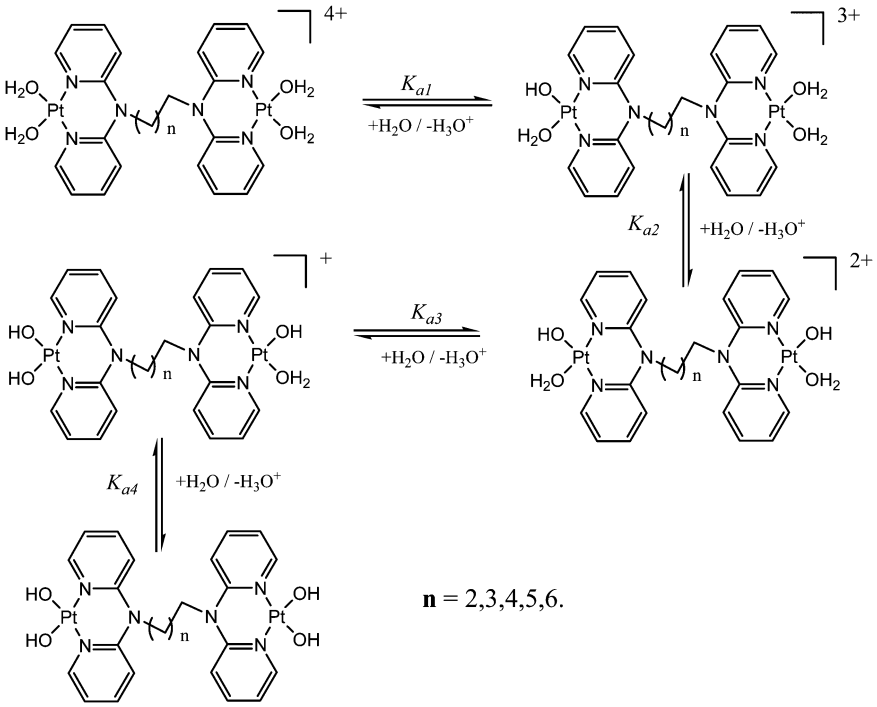

Scheme 2 Proposed stepwise deprotonation of the four aqua ligands on dinuclear Pt(II) complexes.

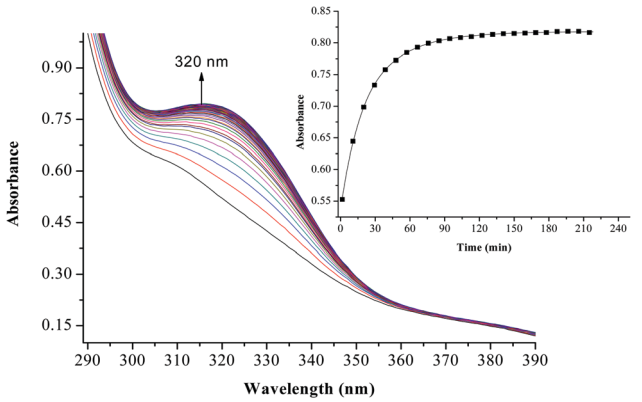

Fig. 3 UV/vis spectral changes observed during the reaction between **PtL3** and TU; the inset is a typical kinetic trace of absorbance *versus* time at 320 nm, T = 298.15 K, pH = 2.0 and I = 0.1 M $NaClO_4$.

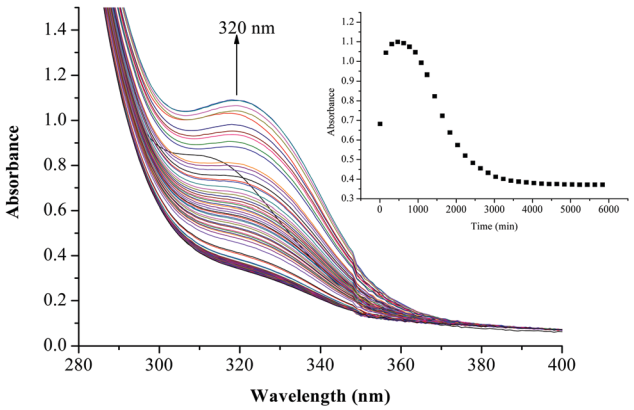

Fig. 4 UV/vis spectral changes observed during the reaction between **PtL6** and TU; the inset is a typical kinetic trace of absorbance *versus* time at 320 nm, T = 298.15 K, pH = 2.0 and I = 0.1 M $NaClO_4$.

in the absorbance at suitable wavelengths as a function of nucleophile concentration and time. Fig. 3 and 4 show typical spectral changes of absorbance *versus* wavelength for the slow reaction steps of complexes with odd and even number of carbons in the alkyl chain of **PtL3** and **PtL6** respectively. The inset is a kinetic trace of absorbance *versus* time from which the pseudo-first-order rate constants k_{obs} were obtained by fitting the single exponential function.

Plots of k_{obs} against nucleophile concentrations resulted in linear dependence second-order rate constants, k_2, with no significant intercepts as shown in Fig. 5, 6 and Fig. S1–S3 in the ESI.† The summary of the second order rate constants is shown in Table 4. Based on this observation, eqn (3) represents the corresponding rate laws for the consecutive reaction steps.

$$k_{obs(1,2,3)} = k_{-2} + k_2[Nu] \approx k_2[Nu] \quad (3)$$

where k_{-2} = rate constant for the solvent path and k_2 = rate constant for the direct path, [Nu] = nucleophile concentration. The contribution of the solvent through the solvolytic path (k_{-2}) is negligible or absent. The values of k_2 obtained from the linear regression analysis from eqn (3) are summarized in Table 4.

Activation parameters

The values of activation parameters $\Delta H^{\#}$ and $\Delta S^{\#}$ are calculated from Fig. 7, 8 and Fig. S4–S7 in the ESI† using eqn (4) below.

$$\ln\left(\frac{k_2}{T}\right) = -\frac{\Delta H^{\#}}{RT} + \left[\ln\left(\frac{k_b}{h}\right)\right] + \frac{\Delta S^{\#}}{R} = \frac{\Delta H^{\#}}{RT} + \left(23.8 + \frac{\Delta S^{\#}}{R}\right) \quad (4)$$

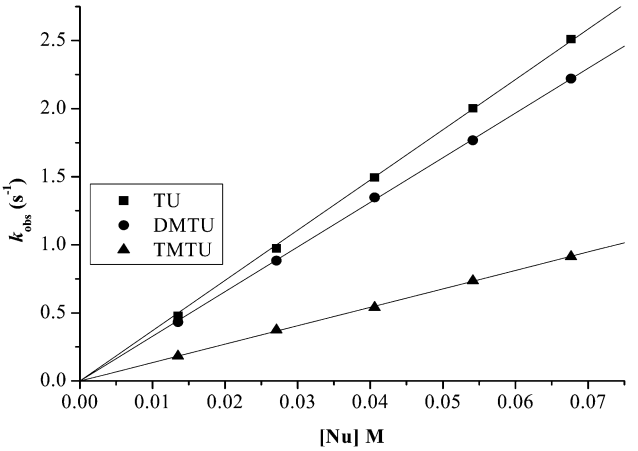

Fig. 5 Plots of $k_{obs(1)}$ *versus* nucleophile concentration for the reaction of **PtL2** at pH = 2.0, T = 298.15 K, I = 0.1 M $NaClO_4$.

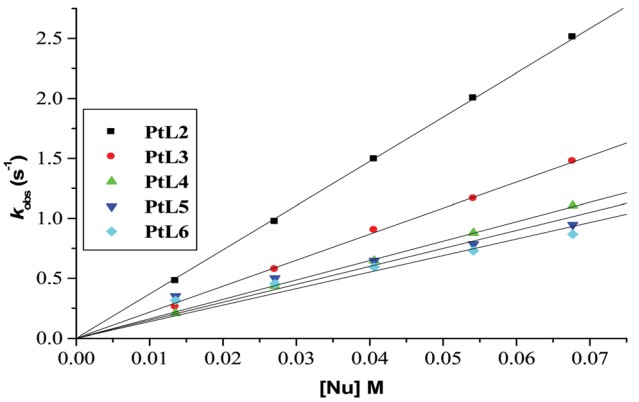

Fig. 6 Plots of $k_{obs(1)}$ *versus* thiourea concentration for the reaction of the dinuclear platinum(II) complexes at pH = 2.0, T = 298.15 K, I = 0.1 M $NaClO_4$.

where k_b and h are Boltzmann's and Planck's constants respectively, T = absolute temperature and R = gas constant. The data for the obtained activation parameters are given in Table 5.

The small but positive $\Delta H^{\#}$ and large negative values of $\Delta S^{\#}$ support an associative mechanism. The low enthalpy values are attributed to bond formation and participation of the entering ligand in the transition state. The large negative values of entropies signify a more compact transition state than that of the reactants.[61]

Substitution reaction

The number of substitution steps was dependent on the "odd or even" effect of the alkyl spacer.[62–64] Complexes with even number of methylene groups [n = 4, 6], **PtL4** and **PtL6**, showed *anti*-conformations (Fig. S32, ESI†) and three kinetic steps were observed except for [n = 2] **PtL2** which showed two reaction steps. On the other hand complexes with odd groups [n = 3, 5], **PtL3** and **PtL5**, showed *syn* conformations with only two reaction steps. These conformations are supported by Albrecht and others who also observed a similar odd–even effect.[65] As such different substitution behaviour is expected due to the different

Table 4 A summary of the second order rate constants, $k_{obs(1,2,3)}$, for displacement of coordinated aqua ligands and the chelation step at pH = 2.0, T = 298.15 K, I = 0.1 M $NaClO_4$

		Second-order rate constant/M^{-1} s^{-1}		
Complex	Nu	$k_{2(1st)}$	$k_{2(2nd)} \times 10^{-2}$	$k_{2(3rd)} \times 10^{-3}$
PtL1*	TU	38.70 ± 0.60	106 ± 3	—
	DMTU	48.80 ± 0.50	2 ± 0.1	—
	TMTU	22.80 ± 0.40	—	—
PtL2	TU	36.90 ± 0.18	4 ± 0.2	—
	DMTU	32.79 ± 0.11	7 ± 0.1	—
	TMTU	13.53 ± 0.06	1 ± 0.1	—
PtL3	TU	21.71 ± 0.22	7 ± 0.1	—
	DMTU	17.43 ± 0.18	3 ± 0.1	—
	TMTU	9.71 ± 0.16	3 ± 0.1	—
PtL4	TU	16.20 ± 0.10	11 ± 0.6	5 ± 0.09
	DMTU	13.57 ± 0.02	6 ± 0.1	3 ± 0.03
	TMTU	7.04 ± 0.08	4 ± 0.06	Too slow
PtL5	TU	10.92 ± 0.14	5 ± 0.02	—
	DMTU	13.45 ± 0.24	3 ± 0.05	—
	TMTU	6.28 ± 0.04	0.8 ± 0.01	—
PtL6	TU	10.21 ± 0.03	8 ± 0.09	0.5 ± 0.02
	DMTU	12.60 ± 0.23	3 ± 0.04	0.7 ± 0.02
	TMTU	5.10 ± 0.04	2 ± 0.04	Too slow

Data for **PtL1*** extracted from ref. 41.

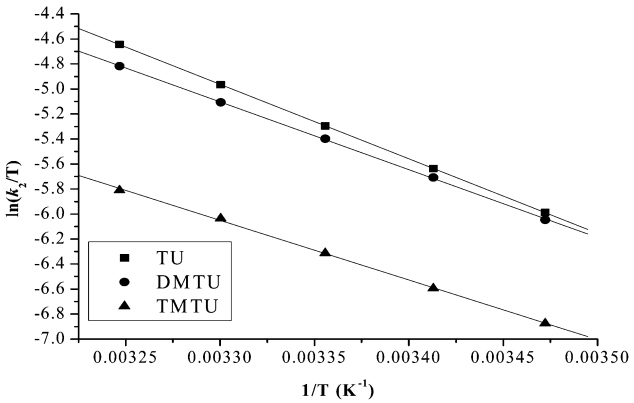

Fig. 7 Eyring plots for the first substitution step of **PtL2** with different nucleophiles at pH = 2.0, I = 0.1 M $NaClO_4$.

architectural framework. The *syn* conformation restricts Pt(II) centres in the same plane making them kinetically equivalent. This equivalency at Pt(II) centres results in simultaneous substitution at the two Pt(II) centres as suggested in this study. The second slow step involves a dechelation after the second water molecule at each Pt(II) centre is substituted. The study shows the displacement of the labilized amine spacer from two Pt(II) ions to occur concurrently. Similar behaviour of a single kinetic step release of two metal ions from the spacer in dinuclear complexes has also been reported by Basollote *et al.*[66]

However, in the *anti*-conformational configuration, the study proposes the first step to be the fast substitution of the water molecule at each Pt(II) centre followed by a slow

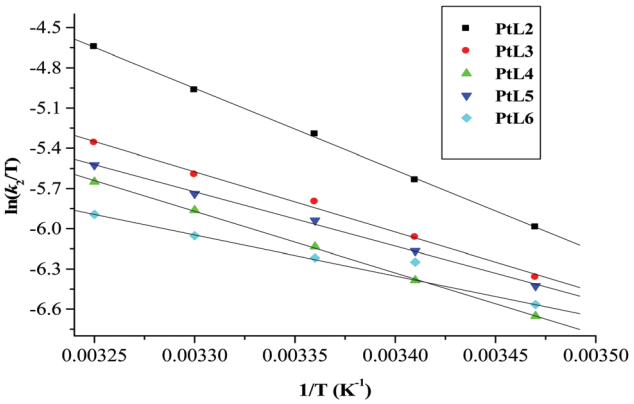

Fig. 8 Eyring plots for the first substitution step of dinuclear platinum(II) complexes with thiourea at pH = 2.0, I = 0.1 M $NaClO_4$.

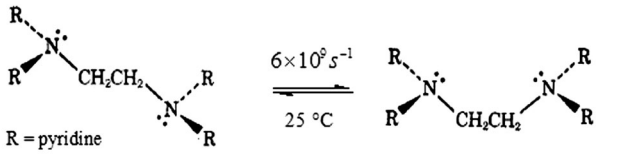

Trans (*anti*-)-conformer *Gauche* (*syn*-)-conformer

Scheme 3 Proposed conformational shifts of **PtL2** as either *trans* or *gauche* conformation.[67]

displacement of the second water molecule that involves the stepwise displacement of the labilized alkyl spacer as a result of the strong *trans* effect of thiourea ligands. However, **PtL2** showed two reaction steps instead of the expected three steps due to its ability to exhibit either *syn*- or *anti*-conformation (Scheme 3). This is partly attributed to its ability to interconvert by rotations around the single bond by approximately 6×10^9 s^{-1} at 25 °C[67] and also due to the shorter spacer between the two Pt(II) centres. Due to the proximity of the metal centres, the study suggests a single kinetic step to release the two metal centres from the spacer.

To show that the complexes undergo a dechelation process, a substitution reaction of the chloride complexes with 6 equivalents of TU was carried out. The reaction products were analyzed using ^1H and ^{195}Pt NMR spectroscopy. The ^{195}Pt NMR spectrum of **PtL6** in DMSO-d_6 at −2175 ppm indicated that the platinum centres were coordinated to two nitrogen atoms (PtN_2Cl_2).[68] Addition of 6 equivalents of TU to the chloride complex solution leads to the shifting of the PtN_2Cl_2 peak from −2175 ppm to −3909.1 ppm. This confirmed the formation of $Pt(TU)_4^{2+}$ complex[69–71] as expected from the *cis* isomer of ($PtNNCl_2$) when reacted with thiourea. The complex reacts completely with thiourea to give $Pt(TU)_4^{2+}$ because of the large *trans* effect as proposed in Scheme 4. The ^1H NMR study shows a σ effect that reduces the electron density from the ligand that leads to a downfield shift. In the ^1H NMR spectrum of complex **PtL6** the alkyl protons (Ha) shift to 1.65 ppm compared to Hb at 1.40 ppm of the ligand (Fig. 9). This downfield shift indicates deshielding of alkyl protons attributed to reduced electron density upon coordination to the metal centre. This decrease in electron density causes alkyl protons to resonate downfield. These shifts support the presence of σ inductive effects causing the shifts of protons of free ligands and their coordinated forms. Due to the *cis* configuration of this class of complexes, the strong *trans*-effect upon coordination to thiourea labilizes the linker that leads to the dechelation as supported by Fig. 9 and 10.

Discussion

The substitution behaviour of dinuclear dipyridylamine Pt(II) complexes with varying alkyl chain lengths was investigated. The kinetic results show that mononuclear 2,2′-dipyridylamine complexes react faster than their dinuclear counterparts. The slow reactivity of dinuclear analogues is due to their increased steric demand compared to mononuclear complexes. In dinuclear

Table 5 Activation parameters for the substitution of aqua ligands by nucleophiles and dissociation of the bridging linker

		Activation enthalpy/kJ mol^{-1}			Activation entropy/J mol^{-1} K^{-1}		
Complex	Nu	$\Delta H_1^{\#}$	$\Delta H_2^{\#}$	$\Delta H_3^{\#}$	$\Delta S_1^{\#}$	$\Delta S_2^{\#}$	$\Delta S_3^{\#}$
PtL2	TU	49.53 ± 0.1	24.41 ± 0.3	—	−76 ± 1	−226 ± 1	—
	DMTU	45.09 ± 0.4	32.52 ± 0.3	—	−92 ± 1	−206 ± 1	—
	TMTU	39.69 ± 0.6	46.12 ± 1.6	—	−117 ± 2	−155 ± 5	—
PtL3	TU	36.53 ± 1.1	23.05 ± 0.1	—	−123 ± 4	−219 ± 1	—
	DMTU	21.01 ± 0.5	40.08 ± 0.5	—	−177 ± 2	−170 ± 2	—
	TMTU	47.39 ± 0.7	37.21 ± 0.6	—	−94 ± 2	−180 ± 2	—
PtL4	TU	37.30 ± 0.6	23.37 ± 0.3	24.16 ± 0.9	−124 ± 2	−218 ± 1	−232 ± 3
	DMTU	39.60 ± 0.4	29.70 ± 0.3	29.57 ± 1.2	−117 ± 1	−205 ± 1	−220 ± 4
	TMTU	39.58 ± 0.5	29.40 ± 1.1	—	−125 ± 2	−201 ± 4	
PtL5	TU	32.90 ± 0.6	44.62 ± 0.5	—	−137 ± 2	−149 ± 2	—
	DMTU	49.54 ± 1.1	46.61 ± 0.8	—	−82 ± 4	−146 ± 3	—
	TMTU	48.93 ± 0.3	30.65 ± 0.4	—	−92 ± 1	−208 ± 1	—
PtL6	TU	24.74 ± 0.2	30.26 ± 0.4	11.55 ± 0.1	−167 ± 1	−194 ± 1	−293 ± 0.1
	DMTU	18.44 ± 0.1	27.02 ± 0.2	22.51 ± 0.3	−189 ± 0.4	−211 ± 1	−255 ± 1
	TMTU	71.15 ± 1.4	43.57 ± 0.5	—	−19 ± 5	−153 ± 2	—

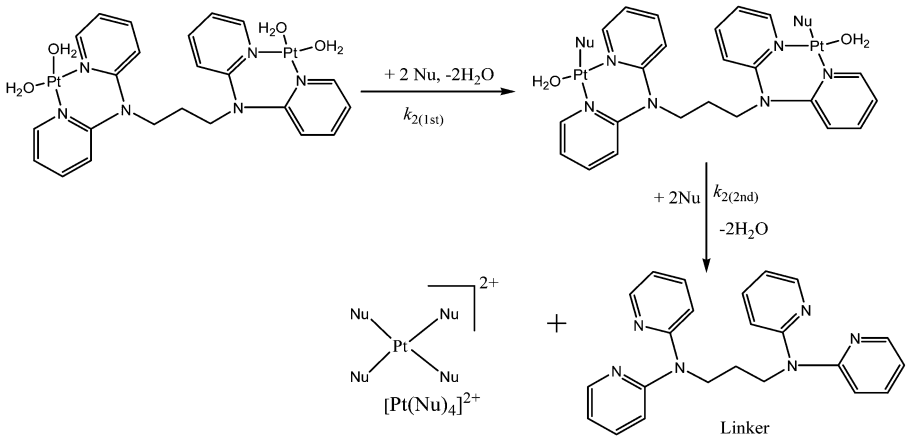

Scheme 4 Proposed substitution mechanism for the odd numbered alkyl chain (n = 3, 5). The $k_{2(3rd)}$ in the even numbered alkyl chain (n = 4, 6) is due to stepwise displacement of the alkyl diamine linker.

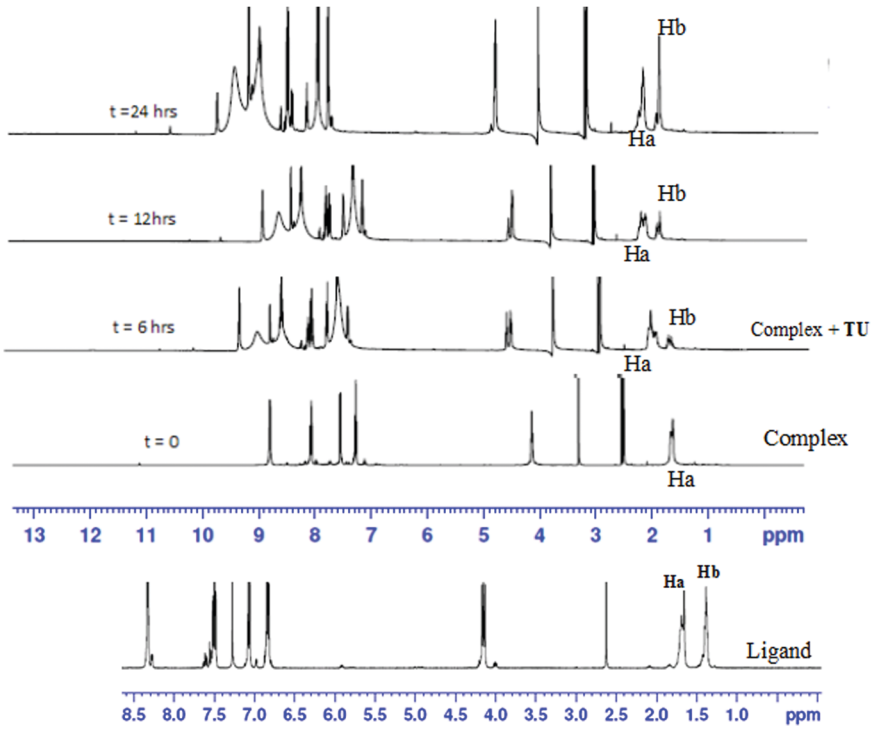

Fig. 9 Time-dependent changes in the ^{1}H NMR spectrum of **PtL6** upon addition of 6 equiv. of TU in DMSO-d_6. The complex undergoes dechelation to form the free ligand (starting material) after 24 h.

complexes, results indicate that the bridging alkyl chain influences the reactivity of the complexes towards the nucleophiles. For the first substitution step, the trend is **PtL1** > **PtL2** > **PtL3** > **PtL4** > **PtL5** > **PtL6** supporting our view on the influence of the chain length. This trend is attributed to the stronger σ-donation as the alkyl chain increases that leads to the stabilization of the metal centres through increased σ-donicity.[72] The longer alkyl groups increase the electron density around the Pt(II) centres through an inductive process. This is enhanced by the lone pair of electrons on the amine nitrogen making them more σ electron donating leading to a decrease in electrophilicity at the metal centres. The electrophilicity of the complexes, **PtL2** (48.44) > **PtL3** (46.96) > **PtL4** (44.74) > **PtL5** (43.49) > **PtL6** (42.09) eV, is in agreement with the reactivity trend. The electronic effect in these complexes is also supported by DFT calculations that shows raised frontier orbitals as the alkyl chain is increased (Table 2). The low lying LUMO orbitals in the short alkyl spacers indicate less σ effect to the dipyridyl rings. This makes complexes with shorter alkyl bridging ligands more reactive towards nucleophilic attack.[73]

However, the HOMO–LUMO energy gap, ΔE, reflects a contradicting trend shown by kinetic data. The Pt(II) complex with the least reactivity, **PtL6**, has the smallest HOMO–LUMO energy gap (ΔE = 4.13 eV) while the most reactive complex, **PtL2**, has the highest energy gap (ΔE = 4.34 eV). Increased

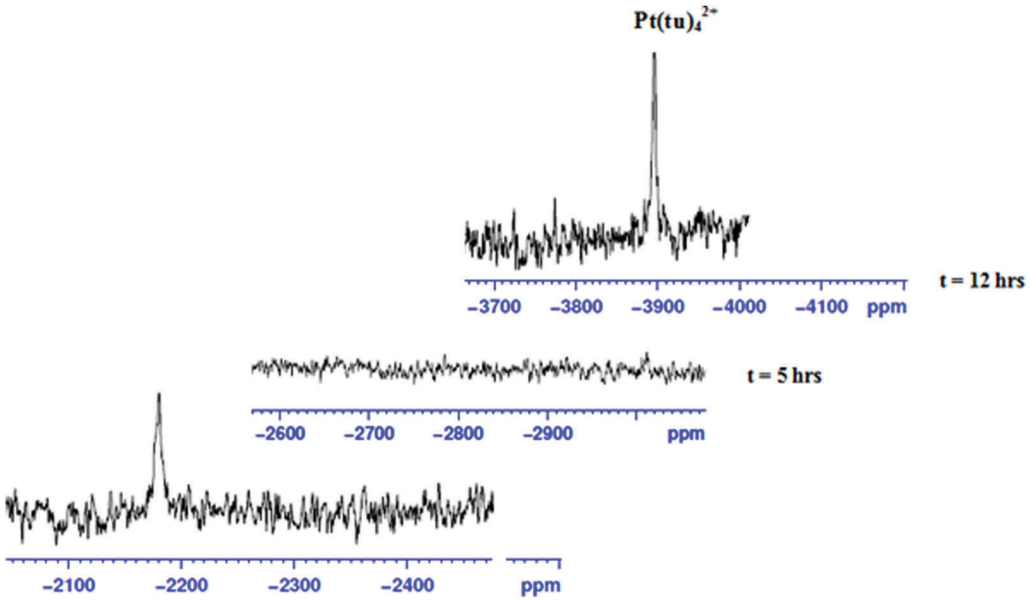

Fig. 10 Time-dependent changes in the ^{195}Pt NMR spectrum of **PtL6;** upon addition of 6 equiv. of TU in DMSO-d_6 the peak at −2175 ppm disappears and reappears at −3909.1 ppm indicating the formation of the [$Pt(TU)_4^{2+}$] complex.[69]

inductive electron donation raises both the HOMO and the LUMO due to the increasing chain length as shown in Fig. 11. This increase in energy is in line with the expectation of electron donating groups to raise the energy of molecular orbitals.

The results obtained from the current study were compared to those of previous works[74,75] where the bis(2-pyridylmethyl)-amine (bpma) head group was appended to alkyl bridges of variable length. The findings in this paper show an opposite trend to those previously reported by Jaganyi and Mambanda.[72] Although both studies used flexible alkyl linkers, the difference is attributed to the different head functionalities at the termini *viz.* bis(2-pyridylmethyl)amine and 2,2′-dipyridylamine. A decrease in the reactivity of 2,2′-dipyridylamine Pt(II) complexes was observed as the $-(CH_2)_n-$ moiety increased due to the linker being in the *cis*-position relative to the leaving group. The trend in the reactivity of this class of bidentate Pt(II) complexes is attributed to the strong σ-ability of the $-(CH_2)_n-$ moiety in the *cis*-position to the leaving group that causes accumulation of electron density around the metal centre. However, this trend is opposite to the kinetic studies reported on the ligand substitution of dinuclear Pt(II) complexes with flexible linkers having bis(2-pyridylmethyl)-amine functionality. This head group forms monodentate dinuclear Pt(II) complexes whose reactivity increases with an increase in chain length due to the *trans*-effect. The high *trans*-effect[76–78] of bis(2-pyridylmethyl)amine linked platinum(II) complexes enhances the rate of substitution through ground state destabilization. This shows the stronger effect of the *trans* ligand to accommodate the excess electronic charge added to the central metal by the entering ligand. By comparing these two studies, they suggest that *cis* ligands are not as effective as *trans* ligands in lowering the activation energy of the ligand → metal σ bonding. This observation is in agreement with classical explanation; the *trans* effect causes electrostatic destabilization of the ligand in the *trans* position. As such, the study supports the fact that the electronic properties of the alkyl spacer dictate the strength of its *trans* effect in the bis(2-pyridylmethyl)amine functionality as the chain length increases. From the two reactivity trends it follows that the *cis* and *trans* effects have an opposite net effect. While the *trans* effect accelerates the rate of substitution through ground state destabilization, the *cis* effect decelerates substitution rates through accumulation of electron density around the metal centre.

This study has shown that the reactivities of dinuclear Pt(II) complexes may be manipulated by the geometry of the complexes ranging from the relationship of the diamine bridge with the leaving group to the nature of the diamine bridge. It further shows that the investigated complexes are stabilized as the alkyl chain increases, a trend that has been previously reported

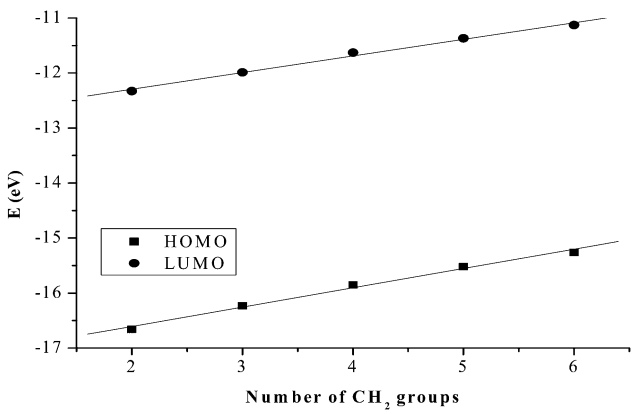

Fig. 11 Linear correlation between the chain length and the HOMO/LUMO orbital energy levels.

by van Eldik[66] and Jaganyi.[79] The stability of the complexes was attributed to stronger σ inductive effects in the *cis* configuration due to the accumulation of electron density around the Pt(II) centre as the alkyl chain increases. From these findings it is concluded that the structural features and reactivity pattern of the investigated dinuclear Pt(II) complexes are governed by both steric and electronic effects arising from the methylene bridge.

Steric factors were influenced by the size of the complex and the preferential conformations of the complexes. Increasing $-(CH_2)_n-$ groups increases the size and flexibility of the complexes resulting in an increased steric hindrance. The slow reactivity of large complexes may partially be attributed to their large size. The study also investigated the reactivity of the entering nucleophiles based on their steric and electronic demands. This investigation shows reactivity to be dependent on the steric influence of the entering nucleophile. The reactivity order of the nucleophiles followed the trend TU > DMTU > TMTU. However, in some cases where DMTU is faster than **TU**, the enhanced reactivity is attributed to the inductive effect by the two methyl groups.[80] The second and third steps are much slower since they are governed by the steric hindrance caused by coordination of the first nucleophile. In cases where the kinetic data are not reported, it was due to the slow reactivity of the nucleophile involved.

Conclusion

This paper has provided a comprehensive investigation on the effect of alkyl chains on the mechanistic substitution reactions of *cis*-dinuclear Pt(II) complexes with tetraaqua ligands. The study shows that the length and parity of the flexible linker are influential parameters on the transitional properties of the metal complexes. The study supports literature findings that the length of the alkyl chain has a significant influence on the structural and electronic properties of the complexes. The kinetic behaviour of the complexes is controlled by the conformations and electronic effect of the alkyl spacers. An increase in alkyl chain length into the Pt(II) coordination sphere results in a decrease in acidity of the coordinated tetraaqua ligands and hence higher stability of the complexes. The results also show the number of substitution steps to be controlled by the odd–even effect of the alkyl spacer. The absence of separate kinetic steps for the release of both Pt(II) ions in the odd numbered alkyl chain suggests an apparent single process of dechelation. The mechanism of substitution is associative in nature as shown by small but positive values of enthalpy and large negative values of entropy. The ability of these complexes to undergo ligand exchange makes them potential candidates for building chemotherapeutic agents for drug delivery. However, the displacement of the labilized chain linker due to the strong *trans* effect by S-donor nucleophiles may limit the application of this family of complexes as anticancer agents. This work has provided a useful approach for tuning the reactivity of new but promising dinuclear platinum anticancer candidates. These results are beneficial in understanding the antitumour activity and toxicity of dinuclear bifunctional Pt(II) complexes. Elucidation of this multilevel mechanism of dipyridylamine Pt(II) complexes with sulphur-donor bio-relevant molecules will greatly increase our understanding of the mechanism of action of bifunctional dinuclear Pt(II) complexes.

Conflicts of interest

There are no conflicts to declare.

Acknowledgements

The authors greatly acknowledge the financial support from the University of KwaZulu Natal. The authors also thank the School of Chemistry and Physics at the University of KwaZulu Natal Pietermaritzburg Campus for support. The authors extend their sincere thanks to Dr Allen Mambanda for his positive criticism and his suggestions to this paper. Last but not least is our appreciation to Mr Craig Grimmer and Miss Janse van Resenburg for NMR, mass and elemental analyses.

References

1 (*a*) P. Gamez, P. de Hoog, O. Roubeau, M. Lutz, W. L. Driessen, A. L. Spek and J. Reedijk, *Chem. Commun.*, 2002, 1488–1498; (*b*) P. Gamez, P. de Hoog, M. Lutz, A. L. Spek and J. Reedijk, *Inorg. Chim. Acta*, 2003, **351**, 319–326.
2 P. de Hoog, P. Gamez, M. Leuken, O. Roubeau, B. Krebs and J. Reedijk, *Inorg. Chim. Acta*, 2004, **357**, 213–218.
3 S. Demeshko, G. Leibeling, S. Dechert and F. Meyer, *Dalton Trans.*, 2004, 3782–3787.
4 C. Seward, W. I. Jia, R. Y. Wang and S. Wang, *Inorg. Chem.*, 2004, **43**, 978–985.
5 W. I. Jia, D. R. Bai, T. McCormick, Q. D. Liu, M. R. Motala, R. Y. Wang, C. Seward, Y. Tao and S. Wang, *Chem. – Eur. J.*, 2004, **10**, 994–1006.
6 E. Wong and C. M. Giandomenico, *Chem. Rev.*, 1999, **99**, 2451–2466.
7 E. R. Jamieson and S. J. Lippard, *Chem. Rev.*, 1999, **99**, 2467–2498.
8 J. Reedijk, *Proc. Natl. Acad. Sci. U. S. A.*, 2003, **100**, 3611–3616.
9 N. J. Wheate and J. G. Collins, *Coord. Chem. Rev.*, 2003, **241**, 133–145.
10 N. Farrell, Y. Qu, U. Bierbach, M. Valsecchi and E. Menta, in *Chemistry and Biochemistry of Leading Anticancer Drug*, ed. Lippert, B., Verlag Helvetica Chimica Acta, Wiley-VCH, Zurich, Weinheim, 1999, pp. 479–496.
11 (*a*) N. Farrell, *Comments Inorg. Chem.*, 1995, **16**, 373–389; (*b*) N. Farrell, in *Platinum and Other Metal Coordination Compounds in cancer Chemotherapy*, ed. S. B. Howell, Plenum Press, New York, 1991, pp. 81–82.
12 E. Raymond, S. Faivre, S. Chaney, J. Woynarowski and E. Cvitkovic, *Mol. Cancer Ther.*, 2002, **1**, 227–235.

13 D. Wong and S. J. Lippard, *Nat. Rev. Drug Discovery*, 2005, **4**, 307–320.
14 J. Kasparkova, J. Novakova, O. Vrana, N. Farrell and V. Brabec, *J. Biol. Inorg. Chem.*, 1999, **38**, 10997–11005.
15 J. Kasparkova, J. Zehnulova, N. Farrell and V. Brabec, *J. Biol. Inorg. Chem.*, 2002, **277**, 48076–48086.
16 J. W. Cox, S. J. Berners Price, M. S. Davies, W. Barlage, Y. Qu and N. Farrell, *Inorg. Chem.*, 2000, **39**, 1710–1715.
17 M. S. Ali, K. H. Whitmire, T. Toyomasi, Z. H. Siddik and A. R. Khokhar, *J. Inorg. Biochem.*, 1999, **77**, 231–238.
18 S. Komeda, M. Lutz, L. A. Spek, M. Chikuma and J. Reedijk, *Inorg. Chem.*, 2000, **39**, 4230–4236.
19 A. J. Kraker, J. D. Hoeschele, W. L. Elliot, H. D. Showalter, A. D. Sercel and N. Farrell, *J. Med. Chem.*, 1992, **35**, 4526–4532.
20 Y. Qu and N. Farrell, *J. Am. Chem. Soc.*, 1991, **113**, 4851–4857.
21 Y. Qu and N. Farrell, *Inorg. Chem.*, 1992, **31**, 930–932.
22 U. Bierbach, Y. Qu, T. W. Hambley, J. Peroutka, H. L. Nguyen, M. Doedee and N. Farrell, *Inorg. Chem.*, 1999, **38**, 3535–3542.
23 N. Farrell, Y. Qu and M. P. Hacker, *J. Med. Chem.*, 1990, **33**, 2179–2184.
24 A. Gund and B. K. Keppler, *Angew. Chem.*, 1994, **106**, 198–2005.
25 R. Mital, T. S. Srivastata, H. K. Parekh and M. P. Chitnis, *J. Inorg. Biochem.*, 1991, **41**, 93–103.
26 H. M. Mansuri-Torshizi, T. S. Srivastata, H. K. Parekh and M. P. Chitnis, *J. Inorg. Biochem.*, 1992, **45**, 135–148.
27 Y. Qu, H. Rauter, A. P. Soares Fontes, R. Bandarage, L. R. Kelland and N. Farrell, *J. Med. Chem.*, 2000, **43**, 3189–3192.
28 R. A. Ruhayel, S. Janina, J. S. Langner, M. J. Oke, S. J. Berners-Price, Z. I. Ibrahim and N. Farrell, *J. Am. Chem. Soc.*, 2012, **134**, 7135–7146.
29 N. Farrell, *Met. Ions Biol. Syst.*, 2004, **41**, 252–296.
30 S. Komeda, Unique platinum-DNA interactions may lead to more effective platinum-based antitumour drugs, *Metallomics*, 2011, **3**, 650–655.
31 J. B. Mangrum and N. Farrell, *Chem. Commun.*, 2010, **46**, 6640–6650.
32 P. Perego, C. Caserini, L. Gatti, N. Carenini, S. Romanelli, R. Supino, D. Colangelo, I. Viano, R. Leone, S. Spinelli, G. Pezzoni, C. Manzotti, N. Farrell and F. Zunino, *Mol. Pharmacol.*, 1999, **55**, 528–534.
33 R. Jarzynka, A. Topolski, M. Uzarska and R. Czajkowski, *Inorg. Chim. Acta*, 2014, **413**, 60–67.
34 J. Reedijk, *Chem. Rev.*, 1999, **99**, 2499–2510.
35 W. E. Curtis, M. E. Muldrow, N. B. Parker, R. Barkley, S. L. Linas and J. E. Repine, *Proc. Natl. Acad. Sci. U. S. A.*, 1988, **85**, 3422–3428.
36 A. A. Shoukry, *J. Chem. Sci.*, 2013, **125**, 643–651.
37 K. Matsumoto, H. Aizawa, H. Inoue, H. Koto, S. Fukuyama and N. Hara, *Eur. J. Pharmacol.*, 2000, **403**, 267–275.
38 P. Pil and S. J. Lippard, Specific Binding of Chromosomal Protein HMGI to DNA Damaged by the Anticancer Drug Cisplatin, *Science*, 1992, **256**, 234–236.
39 B. Petrović, Ž. D. Bugarčić, A. Dees, I. Ivanović-Burmazović, F. W. Heinemann, R. Puchta, S. N. Steinmann, C. Corminboeuf and R. van Eldik, *Inorg. Chem.*, 2012, 1516–1529.
40 M. T. Ashby, *Comments Inorg. Chem.*, 1990, **10**, 297–313.
41 (*a*) S. G. Murray and F. R. Hartley, *Chem. Rev.*, 1981, **81**, 365–441; (*b*) G. Kinunda and D. Jaganyi, *Transition Met. Chem.*, 2016, **41**, 235–248.
42 (*a*) S. Fakih, W. C. Tung, W. D. Eierhoff, C. Mock and B. Krebs, *Z. Anorg. Allg. Chem.*, 2005, **631**, 1397–1402; (*b*) M. J. Rauterkus, S. Fakih, C. Mock, I. Puscasu and B. Krebs, *Inorg. Chim. Acta*, 2003, **350**, 355–365.
43 V.B. Origin7.5™ SRO in Origin Lab Corporation, Northampton, One, Northampton, MA, 01060, USA, 2003.
44 J. Bogojeski, Ž. D. Bugarčić, R. Puchta and R. van Eldik, *Eur. J. Inorg. Chem.*, 2010, 5439–5445.
45 S. Jovanović, B. Petrović, D. Čanović and Ž. D. Bugarčić, *Int. J. Chem. Kinet.*, 2011, **43**, 99–106.
46 N. Summa, W. Schiessl, R. Puchta, R. van Eikema and R. van Eldik, *Inorg. Chem.*, 2006, **45**, 2948–2959.
47 N. Hochreuther, S. T. Nandibewoor, R. Puchta and R. van Eldik, *Dalton Trans.*, 2012, **41**, 512–522.
48 J. D. Atwood, *Inorganic and Organometallic Reaction Mechanisms*, John Wiley & Sons, Canada, 1985, pp. 82–83.
49 M. J. Frisch, G. W. Trucks, H. B. Schlegel, G. E. Scuseria, M. A. Robb, J. R. Cheeseman, G. Scalmani, V. Barone, B. Mennucci, G. A. Petersson, H. Nakatsuji, M. Caricato, X. Li, H. P. Hratchian, A. F. Izmaylov, J. Bloino, G. Zheng, J. L. Sonnenberg, M. Hada, M. Ehara, K. Toyota, R. Fukuda, J. Hasegawa, M. Ishida, T. Nakajima, Y. Honda, O. Kitao, H. Nakai, T. Vreven, J. A. Montgomery, Jr., J. E. Peralta, F. Ogliaro, M. Bearpark, J. J. Heyd, E. Brothers, K. N. Kudin, V. N. Staroverov, R. Kobayashi, J. Normand, K. Raghavachari, A. Rendell, J. C. Burant, S. S. Iyengar, J. Tomasi, M. Cossi, N. Rega, J. M. Millam, M. Klene, J. E. Knox, J. B. Cross, V. Bakken, C. Adamo, J. Jaramillo, R. Gomperts, R. E. Stratmann, O. Yazyev, A. J. Austin, R. Cammi, C. Pomelli, J. W. Ochterski, R. L. Martin, K. Morokuma, V. G. Zakrzewski, G. A. Voth, P. Salvador, J. J. Dannenberg, S. Dapprich, A. D. Daniels, O. Farkas, J. B. Foresman, J. V. Ortiz, J. Cioslowski and D. J. Fox, *Gaussian 09, Revision A.1*, Gaussian, Inc., Wallingford, CT, 2009.
50 (*a*) A. D. Becke, *J. Chem. Phys.*, 1993, **98**, 1372–1377; (*b*) P. J. Stephens, F. Devlin, C. F. Chabalowski and M. J. Frisch, *J. Phys. Chem.*, 1994, **98**, 1623–1627.
51 (*a*) B. Miehlich, A. Savin, H. Stoll and H. Preuss, *Chem. Phys. Lett.*, 1989, **157**, 200–206; (*b*) P. J. Hay and W. R. Wadt, *J. Chem. Phys.*, 1985, **82**, 299–310.
52 C. Lee, W. Yang and R. G. Parr, *Phys. Rev. B: Condens. Matter Mater. Phys.*, 1988, **37**, 785–789.
53 P. W. Asman and D. Jaganyi, *Int. J. Chem. Kinet.*, 2017, **49**, 545–561.
54 P. W. Asman, *Inorg. Chim. Acta*, 2018, **469**, 341–352.
55 P. W. Asman, *J. Coord. Chem.*, 2017, DOI: 10.1080/00958972.2017.1371702.
56 H. Ertürk, A. Hofmann, R. Puchta and R. van Eldik, *Dalton Trans.*, 2007, 2295–2301.

57 (*a*) V. Rai and I. N. N. Namboothiri, *Eur. J. Org. Chem.*, 2006, 4693–4703; (*b*) F. Weinhold and R. L. Clark, *Discovering Chemistry with Natural Bond Orbitals*, John Wiley & Sons, New Jersey, 2012, pp. 132–133.
58 R. Tandon, T. A. Nigst and H. Zipse, *Eur. J. Org. Chem.*, 2013, 5423–5430.
59 (*a*) O. Exner, *J. Phys. Org. Chem.*, 1999, **12**, 265–274; (*b*) M. Charton, *J. Phys. Org. Chem.*, 1999, **12**, 275–282; (*c*) V. Galkin, *J. Phys. Org. Chem.*, 1999, **12**, 283–288; (*d*) O. Exner, M. Charton and V. Galkin, *J. Phys. Org. Chem.*, 1999, **12**, 289–290.
60 H. Stephanie, R. Puchta and R. van Eldik, *Inorg. Chem.*, 2011, **50**, 8984–8996.
61 A. Mandal, P. Karmakar, S. Mallick, B. K. Bera, S. Mondal, S. Ray and A. K. Ghosh, *J. Chem. Sci.*, 2012, **124**, 801–807.
62 G. Pistolis, A. K. Andreopoulou, A. Malliaris and J. K. Kallitsis, *J. Phys. Chem. B*, 2005, **109**, 11538–11543.
63 Y. Qu, N. J. Scarsdale, M. C. Tran and N. Farrell, *J. Biol. Inorg. Chem.*, 2003, **8**, 19–28; Y. Qu, N. J. Scarsdale, M. C. Tran and N. Farrell, *J. Inorg. Biochem.*, 2004, **98**, 1585–1590; Y. Qu, M. C. Tran and N. Farrell, *J. Biol. Inorg. Chem.*, 2009, **14**, 969–977.
64 M. J. Birenne, J. Gabard, M. Leclercq, J. M. Lehn, M. Cesario, C. Pascard, M. Cheve and G. Dutruc-Rosset, *Tetrahedron Lett.*, 1994, **35**, 8157–8167.
65 (*a*) M. Albrecht and S. Kotila, *Angew. Chem., Int. Ed. Engl.*, 1995, **34**, 2134–2137; (*b*) M. Albrecht, *Chem. Soc. Rev.*, 1998, **27**, 281–288; (*c*) M. Albrecht, I. Janser, H. Houjou and R. Frohlich, *Chem. – Eur. J.*, 2004, **10**, 2839–2850; (*d*) M. Albrecht and R. Frohlich, *Bull. Chem. Soc. Jpn.*, 2007, **80**, 797–808; (*e*) C. T. Imrie and P. A. Henderson, *Chem. Soc. Rev.*, 2007, **36**, 2096–2124.
66 M. G. Basallote, J. Durán, M. J. Fernández-Trujillo and M. A. Máñez, *J. Chem. Soc., Dalton Trans.*, 1999, 3817–3823.
67 E. Eliel and H. Wilen, *Stereochemistry of Organic Compounds*, Wiley, New York, 1994, pp. 596–599.
68 B. M. Still, P. G. A. Kumar, J. R. Aldrich-Wright and W. S. Price, *Chem. Soc. Rev.*, 2007, **36**, 665–686.
69 H. Ertürk, R. Puchta and R. van Eldik, *Eur. J. Inorg. Chem.*, 2009, 1331–1338.
70 K. Zamani, A. MobiniKhaledi, N. Foroughifar, K. Faghihi and V. Mahdavi, *Turk. J. Chem.*, 2003, **27**, 71–75.
71 H. Ertürk, J. Magut, R. Puchta and R. van Eldik, *Dalton Trans.*, 2008, 2759–2766.
72 (*a*) D. Reddy and D. Jaganyi, *Int. J. Chem. Kinet.*, 2011, **43**, 161–174; (*b*) A. Hofmann, L. Dahlengburg and R. van Eldik, *Inorg. Chem.*, 2003, **42**, 6528–6538.
73 O. Exner and S. Böhm, *Eur. J. Org. Chem.*, 2007, 2870–2876.
74 A. Mambanda and D. Jaganyi, *Dalton Trans.*, 2011, **40**, 79–91.
75 A. Mambanda, D. Jaganyi, S. Hochreuther and R. van Eldik, *Dalton Trans.*, 2010, **39**, 3595–3608.
76 B. Pinter, V. van Speybroeck, M. Waroquier, P. Geerlings and F. de Proft, *Phys. Chem. Chem. Phys.*, 2013, **15**, 17354–17365.
77 (*a*) C. H. Langford and H. B. Gray, *Ligand Substitution Processes*, W. A. Benjamin, Inc., New York, 1966, vol. 27-33, pp. 79–81; (*b*) F. Basolo, *Mechanisms of Inorganic Reactions*, American Chemical Society, 1965, pp. 23–32.
78 (*a*) B. Coe and S. Glenwright, *Coord. Chem. Rev.*, 2000, **203**, 5–80; (*b*) E. M. Shustorovich, M. Porai-Koshits and Y. Buslaev, *Coord. Chem. Rev.*, 1975, **17**, 1–98.
79 P. O. Ongoma and D. Jaganyi, *Transition Met. Chem.*, 2014, **39**, 407–420; D. Jaganyi, V. M. Munisamy and D. Reddy, *Int. J. Chem. Kinet.*, 2006, **38**, 202–210.
80 D. Jaganyi, F. Tiba, O. Q. Munro, B. Petrović and Ž. D. Bugarčić, *Dalton Trans.*, 2006, 2943–2949.